Semiconductor Physics, Quantum Electronics & Optoelectronics, 2011. V. 14, N 3. P. 375-379.

PACS 73.21.Fg, 73.50.Gr, Pz

Lateral drift of photo-generated charge carriers in the p-SiGe/Si heterostructures with quantum wells

Yu.M. Gudenko[1], V.V. Vainberg[1], V.M. Poroshin[1], V.M. Tulupenko[2]
[1]*Institute of Physics, NAS of Ukraine, 03680 Kyiv, Ukraine*
Phone: 38(044)525-62-58, e-mail: gudenko@iop.kiev.ua
[2]*Donbass State Engineering Academy, 72, Shkadinova str., 84313 Kramatorsk, Ukraine*

Abstract. The drift of charge carriers in the *p*-$Si_{0.88}Ge_{0.12}$/Si heterostructures under strong lateral electric fields and conditions of carrier generation by the band-to-band light absorption has been investigated experimentally. The data of the drift length, drift mobility, and lifetime of charge carriers within the temperature range 20 to 77 K under the electric field up to 1500 V/cm are presented.

Keywords: silicon-based heterostructure, quantum well, lateral transport, strong electric field, photoconductivity.

Manuscript received 30.06.11; accepted for publication 14.09.11; published online 21.09.11.

1. Introduction

The silicon-based heterostructures SiGe/Si are attractive to be used in various functional electronic and optoelectronic devices because of their simple and cheap technology as well as due to possible integration with silicon electronics. There was reported about development of various kinds of transistors [1-4], photodetectors based on intrinsic absorption as well as based on intraband and impurity optical transitions [5-9], lasers for the THz range [10, 11].

Operation of these devices is substantially determined by recombination, diffusion and drift parameters of non-equilibrium charge carriers (NCC). The processes of electron-hole recombination in quantum wells (QWs) of *p*-SiGe/Si heterostructures are sufficiently well investigated (e.g. [12, 13]). At low temperatures the measured lifetimes of NCC in these structures vary from several tenths of nanoseconds to hundreds of microseconds depending on the QW width, germanium fraction, doping profile, impurity concentration, and defect nature. The data on the NNC diffusion length in the *p*-SiGe/Si heterostructures with QWs are given in a lot of published papers (e.g. [14, 15]). However, until now no investigation of the NNC drift in QWs of *p*-SiGe/Si heterostructures under strong lateral electric fields has been carried out.

This paper is devoted to investigation of the lateral drift of photo-generated charge carriers in the *p*-SiGe/Si heterostructures with QWs. The values of the drift length and drift mobility at low temperatures in a wide range of electric fields are given.

2. Samples and experimental techniques

The multilayer heterostructures of *p*-SiGe/Si were grown by the method of molecular beam epitaxy on *n* – Si substrates (100) with the resistivity $\rho \geq 1$ kOhm·cm. (The structures were fabricated in the Center for Condensed Matter Sciences, National Taiwan University, Taipei.) The heterostructures consist of 10 periods containing 15 nm wide SiGe layers, the Ge fraction being of 12 at.% (QWs for holes). The SiGe layers are separated by 10 nm wide Si layers which form barriers for holes and shallow quantum wells for electrons. One part of samples under study was doped by a δ-like impurity layer in the central plane of the SiGe layer, and another part has a δ-impurity at its edge. The impurity concentration in the samples was $6 \cdot 10^{11}$ cm^2 per period. The samples contain also 80-nm wide buffer layers of Si between the substrate and heterostructure, and protecting 40-nm wide cap-layers of Si. The buffer and cap layers were δ-doped by boron with the concentrations $1.3 \cdot 10^{12}$ and $6 \cdot 10^{11}$ cm^{-2}, respectively. The samples were cut to have a rectangular shape with dimensions 8×3 mm. The strip ohmic contacts were made by deposition of Al on their surface and subsequent annealing in vacuum. The distance between contacts was 6.4 mm. The voltage bias from 30 to 1000 V was applied

to the contacts in the pulse regime, the pulse duration and repetition frequency being 3 to 5 μs and 1 Hz, respectively.

The non-equilibrium charge carriers were generated by illumination of a sample surface with a narrow (~500 μm wide) light strip. The photon energy of the light beam was $\hbar\omega$ =1.88 eV (λ = 657 nm) that is wider than the bandgap of the heterostructure layers. The light source was the semiconductor laser ML101J21. The light absorption coefficient in the case under consideration is about $5\times10^3\,\mathrm{cm}^{-1}$. Therefore, for the samples under study the intensity of charge carrier generation is practically constant along their width.

The values of the drift length for charge carriers under the applied lateral electric field $L_{drift}(T,E)$ were determined from the measured dependences of the magnitude of electric current deviation ΔI caused by illumination on the distance between the illuminated area and anode contact, x. Below, for simplicity we refer to ΔI as to the photocurrent.

The lifetime of non-equilibrium charge carriers $\tau(T,E)$ needed in order to determine the bipolar drift mobility $\mu = L_{drift}E/\tau$ was obtained from measurements of photoconductivity decay. In this case, the whole sample surface was illuminated by 3-μs long light pulses with the wavelength λ = 657 nm. The pulse duration of applied electric field in these measurements was 5 to 10 μs.

Measurements were carried out within the temperature range from 10 to 300 K. Within the range ~200 to 300 K, the applied electric field did not exceed 200 V/cm in order to avoid strong Joule heating the samples by a high electric current. At lower temperatures, the measurements were carried out with electric fields up to ~1400 V/cm.

3. Experimental results and discussion

The dependences of photocurrent on the position of illuminated area between contacts have different character in different temperature ranges and at different electric fields applied to the samples. At high temperatures and under all the investigated electric fields, the photocurrent is in fact independent of the light strip position, x, and is the same for both field directions. On the contrary, at low temperatures from 10 to 77 K and electric fields less than approximately 1000 V/cm one observes an increase of photocurrent with increasing distance x. This dependence in the samples doped in the center of QW has a sub-linear behavior, while in the samples doped at the edge of QW it is super-linear. A typical view of these dependences is presented in Fig. 1. It should be noted that switching the field direction applied to a sample to the opposite one leads only to a mirror inversion of dependences described above in regard to x. This gives evidence that they are determined by lateral transport of non-equilibrium charge carriers and are not caused by inhomogeneity of a structure between contacts.

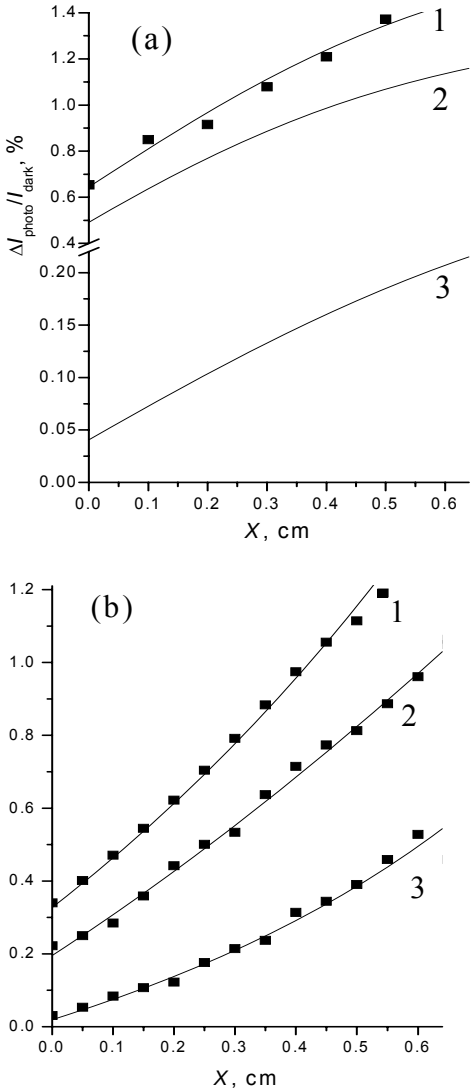

Fig. 1. Profiles of ratio of the photocurrent and dark current under moderate electric fields: (a) on-center doped sample: *1* – T = 23 K, *2* – 30 K, *3* – 77 K, E = 550 V/cm; (b) on-edge doped sample: *1* – T = 25 K, *2* – 35 K, *3* – 77 K, E = 550 V/cm. Squares – experiment, solid lines – fitting.

At higher electric fields, the photocurrent first increases with increasing the distance between the illuminated area and anode, x. Then, beginning from some distance ΔI becomes constant (Fig. 2). The range of x, where photocurrent is constant, becomes shorter with increase of electric field at a constant temperature.

It is natural to relate the observed difference in behavior of photocurrent induced by illumination of a part of a sample with different distributions of photo-generated electrons and holes along the sample between contacts. In a general case, it is determined by diffusion and drift of charge carriers. At higher temperatures and small fields, when the main role in transport of carriers is played by diffusion, the distribution of carriers in both directions from the illuminated strip is symmetrical, the concentration decay along the sample being exponential

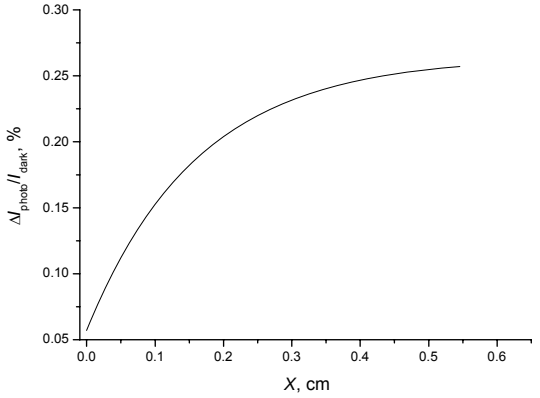

Fig. 2. A typical profile of ratio of the photocurrent and dark current under strong electric fields: $T = 40$ K, $E = 1125$ V/cm. Squares – experiment, solid line – fitting.

and the bipolar diffusion length L_{diff} being a characteristic decay length [16]. If L_{diff} is much less than the distance between electric contacts then the photocurrent magnitude does not depend on the position of the illuminated strip because at any x the carriers do not reach contacts. At temperatures 200 to 300 K, this condition is fulfilled since the diffusion length is about 30 μm. On the contrary, at lower temperatures already under moderate fields the drift begins to play the main role. The distribution of non-equilibrium carriers becomes asymmetric and its concentration occurs larger in direction to the anode contact which corresponds to the drift direction of minority carriers, i.e., electrons in our case. It is easy to show that in case the bipolar drift length L_{drift} is longer than the bipolar diffusion length L_{diff}. The relationship between the photocurrent and position of the illuminated strip between contacts is as follows

$$\Delta I_{photo} \approx I_{dark} \frac{L_{drift}}{L} \times \times \left[\frac{x}{L_{drift}} - \ln\left(a + \exp\frac{x}{L_{drift}} \right) + \ln(1+a) \right], \quad (1)$$

where a is the fitting parameter.

As it follows from Eq. (1), the value of ΔI_{photo} increases with increasing the distance x, while x does not exceed the drift length L_{drift}. When x exceeds L_{drift} in Eq. (1), the value ΔI_{photo} becomes independent of x. It is this behavior that was observed in our experiments.

Fitting of experimental dependences $\Delta I_{photo}/I_{dark}(x)$ by Eq. (1) is shown in Figs 1 and 2. Satisfactory agreement between calculations and experiment is achieved with a suitable choice of the fitting parameter a and drift lengths, which are shown in Fig. 3 for different values of electric field strength. As it is seen from Fig. 3, the drift length in the temperature range under study has a weak dependence on temperature. Moreover, its dependence on the electric field strength is non-monotonous. It is indicative of the fact that the bipolar drift mobility and lifetime of carriers depend on the field value.

Fig. 4 shows results of measurements of the carrier lifetime τ at different values of the lateral electric field and temperatures below 30 K. These data give evidence that, in the studied temperature range, τ in the structures under consideration is practically independent of temperature, and its value is about 2.5×10^{-7} s at low fields. This value is within the interval of lifetimes observed in such structures earlier and corresponds to recombination via impurity centers [12, 13]. With increasing electric fields, the lifetime of NCC, τ, somewhat increases that may be related with a decreasing possibility for carriers to be captured by impurities due to an increase of their average energy in the field.

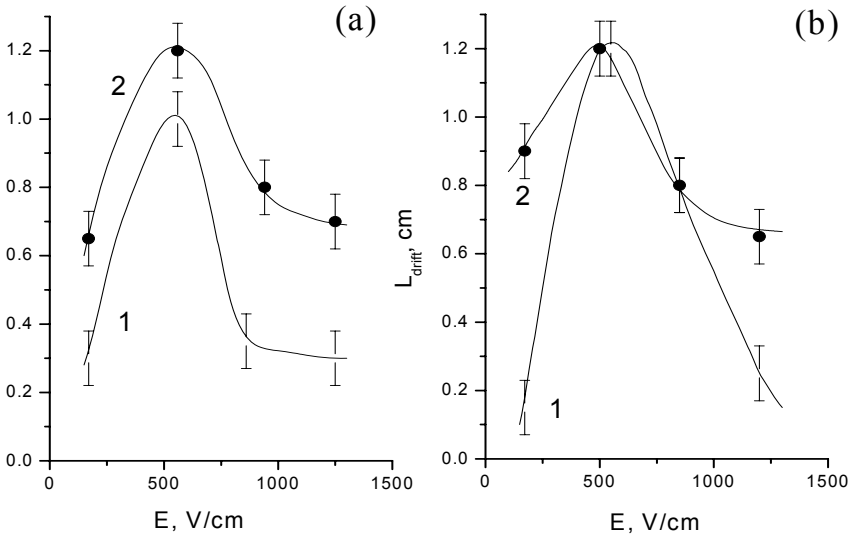

Fig. 3. Dependences of the drift length on the electric field: (a) on-center doped sample, *1* – $T = 25$ K, *2* – 30 K; (b) on-edge doped sample, *1* – $T = 25$ K, *2* – 35 K.

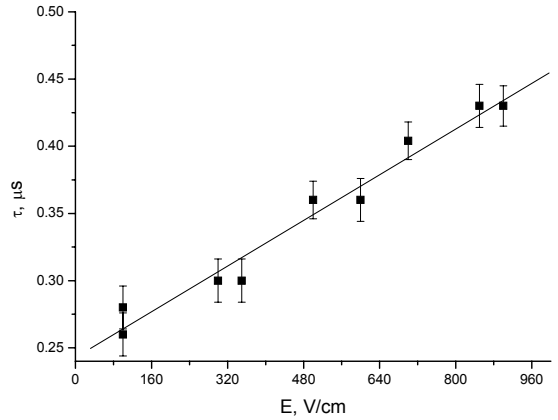

Fig. 4. Typical dependences of the lifetime of non-equilibrium charge carriers on the electric field at temperatures below 30 K.

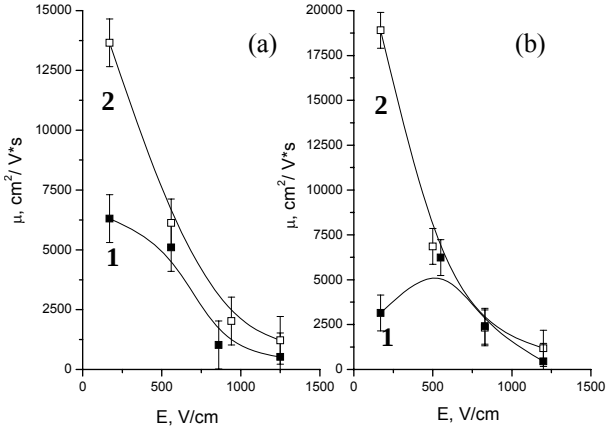

Fig. 5. Field dependences of the bipolar mobility at different temperatures: (a) on-center δ-doped structure: *1* – T = 25 K, *2* – 30 K; (b) on-edge δ-doped structure: *1* – T = 25 K, *2* – 35 K.

The obtained values of the drift length and lifetime of carriers were used to determine the bipolar drift mobility μ at different values of electric field and temperature. The results are shown in Fig. 5 for structures doped both in the center and at the edge of QW. Under low electric fields, the mobility increases with growing temperature that is characteristic for impurity scattering of carriers. It should be noted that at the same temperature the mobility in the on-edge doped samples is higher as compared to the center-doped ones. A mobility increase with moving impurity position from the center to the edge of QW is caused by decreasing impurity scattering. The latter is caused by a decrease of overlapping extent of enveloping wave functions of charge carriers in the size-quantized subband with ionized impurity atoms.

Fig. 5 shows that the bipolar drift mobility of carriers decreases with increasing the electric field value. It may be explained only by contribution of more heavy holes to conduction in the higher subbands of QW due to their occupation caused by heating the holes up by electric field. As follows from our calculations, the hole effective mass in the first, second and third subbands in the structures under study is $0.26m_0$, $0.32m_0$, $0.41m_0$ (m_0 is the free electron mass), respectively.

4. Conclusions

Thus, for the SiGe/Si heterostructures with delta-doped quantum wells we have determined the drift length of non-equilibrium charge carriers under the lateral electric fields within the temperature range 20 to 77 K. It has been shown that the non-linear dependence of the drift length on the magnitude of electric field is caused by the field dependences of charge carrier mobility and lifetime. The observed decrease of bipolar mobility under strong electric fields is explained by transitions of holes to the second size-quantized subband in the quantum well due to heating by field, where they have a higher effective mass.

Acknowledgements

The authors are grateful to Prof. O.G. Sarbey for helpful discussion.

References

1. I. Shahnovich, Solid state UHF devices and technologies. Current state and perspectives // *Electronics: Science, Technology, Busyness*, **5**, p. 58-64 (2005).
2. E.A. Fitzgerald, Ch.W. Leitz, M.L. Lee, D.A. Antoniadis, M.T. Currie, Si industry at a crossroads: New materials or new factories? // *Advanced Materials for Micro- and Nano-Systems (AMMNS)*, **01** (2002).
3. D.J. Paul, Si/SiGe heterostructures: from material and physics to devices and circuits // *Semicond. Sci. Technol*. **19**, p. R75-R108 (2004).
4. A. Zaslavsky, S. Luryi, C.A. King, and R.W. Johnson, Multi-emitter Si/SiGe heterojunction bipolar transistor with no base contact and enhanced logic functionality // *IEEE Electron. Device Lett.*, **18**(9), p. 453-455 (1997).
5. Po-Hsing Sun, Shu-Tong Chang, Yu-Chun Chen, and Houngchin Lin, A SiGe/Si multiple quantum well avalanche photodetector // *Solid State Electron*., **54**(10), p. 1216-1220 (2010).
6. A. Elfving, A. Karim, G.V. Hansson, and W.-X. Ni, Three-terminal Ge dot/SiGe quantum-well photodetectors for near-infrared light detection // *Appl. Phys. Lett*. **89**, 083510-083513 (2006).
7. P. Rauter, G. Mussler, D. Grutzmacher, and T. Fromherz, Tensile strained SiGe quantum well infrared photodetectors based on light-hole ground state // *Appl. Phys. Lett*. **98**, 211106-211109 (2011).

8. C.-H. Lin, C.-Y. Yu, P.-S. Kuo, C.-C. Chang, T.-H. Guo, and C.W. Liu, Δ-doped MOS Ge/Si quantum dot/well infrared photodetector // *Thin Sold Films*, **508** (1-2), p. 389-392 (2006).
9. Fei Liu, Song Tong, Hyung-jun Kim, Kang K. Wang, Photoconductive gain of SiGe/Si quantum well photodetectors // *Optical Materials,* **27**, p. 864-867 (2005).
10. V. Altukhov, E.G. Chirkova, V.P. Sinis et al., Toward $Si_{1-x}Ge_x$ quantum well resonant-state terahertz laser // *Appl. Phys. Lett*. **79**, p. 3809 (2001).
11. M.S. Kagan, I.V. Altukhov, E.G. Chirkova et al., THz lasing of SiGe/Si quantum well structures due to shallow acceptors // *Phys. Status Solidi* (*b*), **235** (1), p. 135-138 (2003).
12. E. Dekel, E. Ehrenfreund, D. Gershoni, P. Boucaud, I. Sagnes and Y. Campidelli, Recombination processes in SiGe/Si quantum wells measured by photoinduced absorption spectroscopy // *Phys. Rev. B*, **56** (24), p. 15734-15739 (1997).
13. E. Corbin, C.J. Williams, K.B. Wong, R.J. Turton, and M. Jaros, Optical spectra and recombination in Si-Ge heterostructures // *Thin Sold Films*, **294** (1-2), p. 186-189 (1997).
14. L.K. Bera, Shajan Mthew, N. Balasubramanian et al., Analysis of carrier generation lifetime in strained-Si/SiGe heterojunction MOSFETs from capacitance transient // *Appl. Surf. Sci.*, **224**, p. 278 (2004).
15. P.V. Schwartz, J.C. Sturm, Microsecond carrier lifetimes in strained silicon-germanium alloys grown by rapid thermal chemical vapor deposition // *Appl. Phys. Lett.* **57**, p. 2004 (1990).
16. S.M. Ryvkin, *Photoelectric Phenomena in Semiconductors*. Fizmatlit, Moscow, 1963 (in Russian).